Transp Porous Med (2010) 83:233–256
DOI 10.1007/s11242-010-9533-8

An Asymptotic Model of Seismic Reflection from a Permeable Layer

Dmitriy Silin · Gennady Goloshubin

Received: 6 November 2009 / Accepted: 17 January 2010 / Published online: 9 February 2010

Abstract Analysis of compression wave propagation in a poroelastic medium predicts a peak of reflection from a high-permeability layer in the low-frequency end of the spectrum. An explicit formula expresses the resonant frequency through the elastic moduli of the solid skeleton, the permeability of the reservoir rock, the fluid viscosity and compressibility, and the reservoir thickness. This result is obtained through a low-frequency asymptotic analysis of Biot's model of poroelasticity. A review of the derivation of the main equations from the Hooke's law, momentum and mass balance equations, and Darcy's law suggests an alternative new physical interpretation of some coefficients of the classical poroelasticity. The velocity of wave propagation, the attenuation factor, and the wave number are expressed in the form of power series with respect to a small dimensionless parameter. The absolute value of this parameter is equal to the product of the kinematic reservoir fluid mobility and the wave frequency. Retaining only the leading terms of the series leads to explicit and relatively simple expressions for the reflection and transmission coefficients for a planar wave crossing an interface between two permeable media, as well as wave reflection from a thin highly permeable layer (a lens). Practical applications of the obtained asymptotic formulae are seismic modeling, inversion, and attribute analysis.

Keywords Hooke's law · Darcy's law · Poroelasticity · Low frequency · Permeability · Asymptotic analysis · Seismic imaging

This work is dedicated to the memory of V. M. Entov.

D. Silin (✉)
Lawrence Berkeley National Laboratory, 1 Cyclotron Road, MS 90R1116, Berkeley, CA 94720, USA
e-mail: DSilin@lbl.gov

G. Goloshubin
University of Houston, 312 Science and Research Bldg 1, Houston, TX 77204-5006, USA
e-mail: ggoloshubin@uh.edu

1 Introduction

The classical theory of elasticity associates anomalously high reflection from a layer in a homogeneous medium with the tuning effect, which takes place when the thickness of the layer is equal to one-fourth of the wavelength (White 1983). However, field observations demonstrate anomalous seismic signal reflection from a thin fluid-saturated permeable layer in the low-frequency end of the spectrum, where the thickness of the reservoir is much smaller than a quarter of the wavelength. Moreover, frequency-dependent data analysis identifies the most productive spots in the reservoir (Goloshubin and Bakulin 1998; Goloshubin and Korneev 2000; Goloshubin et al. 2001, 2002, 2006, 2008; Castagna et al. 2003; Goloshubin and Silin 2005; Wei et al. 2009). In this study, we explain this seemingly abnormal reflection by the interaction between the elastic wave and fluid flow.

The theoretical foundations of seismic wave propagation in a fluid-saturated porous medium have been established in the pioneer works by Frenkel, Gassmann, Biot, and others (Frenkel 1944; Gassmann 1951; Biot 1956a,b; Kosachevskii 1961; Geertsma and Smit 1961; Deresiewicz and Rice 1962). Nikolaevskii, see Nikolaevskii (1996) and Nikolaevskii et al. (1970), has developed a comprehensive theory of coupling between deformation, flow, and heat transfer in porous media. Overviews of the Frenkel, Gassmann, and Biot theories and further development of poroelasticity are presented in Nikolaevskii, see Nikolaevskii et al. (1970), Berryman (1982, 1999), Pride (2005), and Pride and Garambois (2005). Extensions accounting for local heterogeneities including double-porosity or layered media have been developed in Gurevich (1997), Carcione (1998, 2003), Berryman and Wang (2000), Pride and Berryman (2003a,b), and Helle et al. (2003). The reflection and transmission coefficients predicted by Biot's theory for a wave crossing a planar interface have been calculated in Dutta and Ode (1983), Gurevich et al. (2004) and Vikhorev et al. (2005). The complexity of the expressions for the reflection and transmission coefficients derived from the exact Biot's solution makes unclear what is the relative impact of the rock and fluid properties on the magnitudes of the reflection and transmission coefficients. On the contrary, the simplified low-frequency asymptotic relationships obtained in this study yield approximate but relatively simple and practically useful expressions for the reflection and transmission coefficients.

The small parameter used in the asymptotic analysis below is equal to the product of the reservoir fluid mobility and density, and the frequency of the signal, multiplied by an imaginary unit. The velocities of the slow and fast Biot's waves, and the respective wave numbers and attenuation factors are expressed as power series with respect to this small parameter. The coefficients of the series are real-valued functions of the properties of the reservoir rock and fluid. Retaining only the leading terms of the series produce relatively simple mathematical expressions, which are valid in the low-frequency end of the spectrum including the seismic frequency band (10–100 Hz). Using these expressions, we study the reflection and transmission coefficients for a planar wave crossing a permeable interface at a normal incident angle. We further obtain that the fast-wave reflection coefficient from a thin permeable layer (a lens) attains a peak value. The corresponding peak frequency is expressed through the reservoir rock and the fluid properties. The magnitude of this frequency predicted by the obtained formulae is in agreement with the field observations (Goloshubin et al. 2006, 2008). The practical implications of the theory developed here are seismic modeling, inversion, and attribute analysis.

We review the equations of poroelasticity by relating them to Darcy's law, Hooke's law, and momentum and mass balance equations. Although the obtained equations are essentially the same the original Biot's equations (Biot 1956a,b), our approach provides new physical interpretations of some poroelasticity coefficients. For instance, we demonstrate that the

Biot–Willis coefficient α (Biot and Willis 1957) is related to the relative surface area of the grains, which is not exposed to the fluid. Gassmann's results (Gassmann 1951) appear as the zero-frequency limit of the asymptotic solution presented in this study.

We assume that the deformations are small and the macroscopic stress–strain relationship for the skeleton are adequately described by the Hooke's law (Landau and Lifschitz 1986). We have to modify Darcy's law to account for dynamic and nonequilibrium effects in fluid flow. We demonstrate that this modification of Darcy's law is equivalent to a linearization of the dynamic permeability discussed in Johnson et al. (1987), Cortis (2002), and Carcione (2003) for a periodic oscillatory flow. The dynamic component of the modified Darcy's law does not enter the leading terms of the asymptotic expressions. Thus, we conclude that the classical Darcy's law formulation (Darcy 1856; Hubbert 1940, 1956; Barenblatt et al. 1990) is sufficient for the low-frequency analysis.

This study, to a certain degree, is an extension of the work (Silin et al. 2006). Besides a slightly different choice of the small parameter, we abandon the assumption of grain stiffness employed in Silin et al. (2006). More importantly, in the study of reflection and transmission coefficients for a *permeable* interface.

This article is organized as follows. In Sect. 2, we briefly overview the derivation of the equations of poroelasticity from the basic theoretical principles of flow and deformation in porous media. In Sect. 3, we obtain an asymptotic harmonic-wave solution valid in the low-frequency range. In Sect. 4, we obtain explicit expressions for the reflection and transmission coefficients for a planar compression wave crossing a permeable interface. The resonant frequency of a fast wave reflection from a permeable layer is studied in Sect. 5. Finally, Sect. 6 summarizes the findings and formulates the conclusions.

2 The Model

Throughout this study, the porous medium is assumed to be homogeneous and isotropic, and the fluid is newtonian. The linear dimensions of an elementary volume of the medium are small relative to the linear dimensions of the entire medium, but large relative to the size of individual pores or grains constituting the solid skeleton. The total stress in bulk medium is the resultant of three components: the elastic stress in the solid skeleton, the fluid pressure, and viscous friction in the fluid flow relative to the solid skeleton. In a linear approximation, these components are decoupled; so they can be considered separately and then summed up.

2.1 Linear Elasticity of Drained Skeleton

The macroscopic stress in the drained skeleton σ_s is a bulk-area average of the grain-to-grain contact forces, Fig. 1. Let $\mathbf{u} = (u_x, u_y, u_z)$ denote the vector of macroscopic displacement of the solid skeleton and $\Xi = \{u_{ij}\}$ denote the macroscopic strain tensor:

$$u_{11} = \frac{\partial u_x}{\partial x},\ u_{12} = \frac{1}{2}\left(\frac{\partial u_x}{\partial y} + \frac{\partial u_y}{\partial x}\right),\ u_{13} = \frac{1}{2}\left(\frac{\partial u_x}{\partial z} + \frac{\partial u_z}{\partial x}\right),\ \text{etc.} \tag{1}$$

The Hooke's law for an isotropic and uniform medium says:

$$\sigma^s = K\nabla\cdot\mathbf{u}I + 2\mu\left(\Xi - \frac{1}{3}\nabla\cdot\mathbf{u}I\right) \tag{2}$$

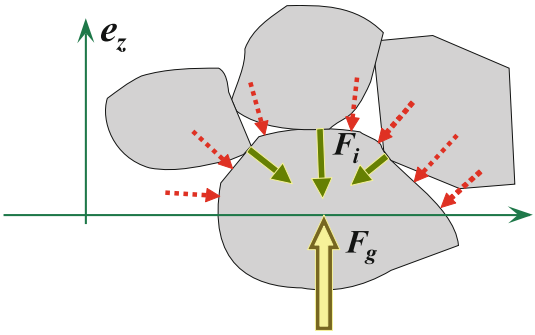

Fig. 1 Force balance at an individual grain in a clean rock. The force $\mathbf{F}_g$ at a plane cross-section orthogonal to a unit normal $\mathbf{e}_z$ equals the sum of contact forces $\mathbf{F}_i$ shown as *solid arrows*, and fluid pressure acting at the part of the grain surface in located the positive with respect to $\mathbf{e}_z$ half-space, shown as *dashed arrows*

where K and μ are the bulk and shear moduli of the drained skeleton, respectively, and I is an identity tensor (Landau and Lifschitz 1986). Note that the macroscopic skeleton moduli are different from the bulk and shear moduli of the grain material.

2.2 Fluid Pressure

In order to evaluate the fluid pressure contribution to the total stress, consider forces acting in the planar cross-section, which Fig. 1 displays as the horizontal axis. We assume that the cross-section intersects sufficiently many grains. The fluid pressure portion of the total stress includes two components: the pore pressure and the portion of the stress in the skeleton which is the reaction on the pore pressure. Inside the pores, the fluid pressure contribution amounts to $p\phi$, where p denotes the pressure of the fluid and ϕ is the porosity of the medium. In an individual grain, the fluid pressure acts through the grain surface. In general, only a portion of this surface is exposed to the fluid, whereas the remaining part is excluded from the fluid–solid interaction by the contacts with the neighbor grains. The force $\mathbf{F}_g$ in Fig. 1 equilibrates the sum of contact forces, $\mathbf{F}_i$, and the integral of the pressure over the portion of the grain surface which is in contact with the pore fluid. Summing up over all grains in the cross-section, the total action of the fluid pressure inside the skeleton is characterized by $(1-\phi)\alpha_\phi p$, where α_ϕ is a dimensionless geometric factor accounting for the portion of the average portion of the grain surface, which is excluded from a contact with the fluid. Clearly, $0 \le \alpha_\phi \le 1$. After adding $p\phi$, the pore pressure contribution in the pores, one obtains:

$$\sigma^{\mathrm{p}} = -\alpha p I \tag{3}$$

where $\alpha = \phi + \alpha_\phi(1-\phi)$, and σ^{p} is the entire pore pressure contribution to the total stress. Note that $\phi \le \alpha \le 1$. The two extreme values of α are $\alpha = 1$ and $\alpha = \phi$. The first one describes a medium where the average grain-to-grain contact area is negligibly small, for example in unconsolidated sand. The other extreme case can be represented by a medium where the skeleton is a bundle of infinite cylindrical columns.

The argument above is not new; our approach is similar to that developed in Khristianovich and Kovalenko (1991).

2.3 Fluid Flow

If the skeleton moves with a constant acceleration, then Darcy's law for the flow relative to the skeleton can be written in the form:

$$\frac{\eta}{\kappa}\mathbf{W} = -\nabla p - \varrho_{\mathrm{f}}\frac{\partial^2 \mathbf{u}}{\partial t^2} \tag{4}$$

where $\mathbf{W}$ denotes the Darcy velocity of the fluid relative to the skeleton, η and ϱ_{f} denote fluid viscosity and density, respectively, and κ is the absolute permeability of the medium. The left-hand side expresses the viscous drag force acting between the fluid and the solid skeleton, whereas the second term on the right-hand side accounts for the body force acting on the fluid in a non-inertial reference frame associated with the skeleton. Equation 4 is an expression of force balance. In an oscillating system, the fluid flows relative to the skeleton with an acceleration. Therefore, the body force on the right-hand side of Eq. 4 must include an additional term $\varrho_{\mathrm{f}}\frac{1}{\phi}\frac{\partial \mathbf{W}}{\partial t}$. In addition, the steady flow paths in the tortuous pore channels establish not instantaneously, the drag force on the left-hand side depends not only on the instantaneous Darcy velocity, but also on its variation. In a linear approximation, we write

$$\frac{\eta}{\kappa}\left(\mathbf{W} + \tau_* \frac{\partial \mathbf{W}}{\partial t}\right) = -\nabla p - \varrho_{\mathrm{f}}\frac{\partial^2 \mathbf{u}}{\partial t^2} - \varrho_{\mathrm{f}}\frac{1}{\phi}\frac{\partial \mathbf{W}}{\partial t} \tag{5}$$

where τ_* is a parameter having the dimensionality of time. Thus, finally, one obtains:

$$\mathbf{W} + \tau \frac{\partial \mathbf{W}}{\partial t} = -\frac{\kappa}{\eta}\left(\nabla p + \varrho_{\mathrm{f}}\frac{\partial^2 \mathbf{u}}{\partial t^2}\right) \tag{6}$$

where parameter $\tau = \tau_* + \frac{\kappa \varrho_{\mathrm{f}}}{\eta \phi}$ accounts both for the nonequilibrium effects of nonsteady fluid flow and fluid inertia. We will call Eq. 6 *dynamic* Darcy's law. If the motion of the skeleton can be neglected, Eq. 6 reduces to the model of filtration with relaxation (Alishaev and Mirzadzhanzadeh 1975). If, in addition, the flow is steady, Eq. 6 yields the classical Darcy's law (gravity is neglected throughout this study).

Different Darcy's law modifications accounting for dynamic and nonsteady effects have been developed in the past and are discussed below, after deriving the asymptotic low-frequency solution. Equation 6 with $\tau_* = 0$ has been obtained by Frenkel (1944), Nikolaevskii, see Nikolaevskii et al. (1970), and Nikolaevskii (1996). We have found the form of Eq. 6 most convenient for the low-frequency asymptotic analysis below. This analysis shows that the parameter τ enters only the higher-order terms. In other words, one can assume $\tau = 0$ in the low-frequency end of the spectrum.

2.4 Flow-Imposed Shear Stress

A shear wave preserves the volume and porosity, and does not affect the pore pressure. The viscose friction between the fluid flowing in the pores and the skeleton develops a distributed drag force proportional to the Darcy velocity of the fluid relative to the skeleton. The Darcy velocity is orthogonal to the wave propagation, see Fig. 2. Interaction of the porous layer between planes with coordinates x and $x + \mathrm{d}x$ with the rest of the formation includes the shear stress in the skeleton, and the drag force by the fluid flowing relative to the skeleton on both sides of the layer. Since the Darcy velocities of the fluid at the two sides of the layer are different, the drag forces are different as well. Therefore, in addition to the shear stress in the skeleton, there is a component coming from the Darcy velocity variation in direction orthogonal to the wave propagation. We denote this stress by σ^{f}.

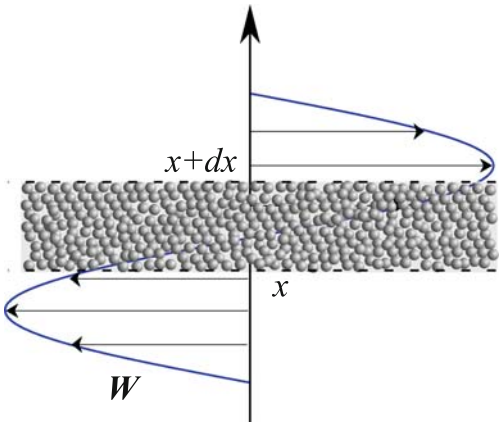

Fig. 2 Darcy velocity direction and variation in a shear wave propagating in direction x

More generally, the shear stress σ^{f} is a linear function of the following tensor:

$$\sigma^{\mathrm{f}} = -\varphi \begin{pmatrix} 0 & \frac{\partial W_y}{\partial x} + \frac{\partial W_x}{\partial y} & \frac{\partial W_x}{\partial z} + \frac{\partial W_z}{\partial x} \\ \frac{\partial W_y}{\partial x} + \frac{\partial W_x}{\partial y} & 0 & \frac{\partial W_y}{\partial z} + \frac{\partial W_z}{\partial y} \\ \frac{\partial W_x}{\partial z} + \frac{\partial W_z}{\partial x} & \frac{\partial W_y}{\partial z} + \frac{\partial W_z}{\partial y} & 0 \end{pmatrix} \tag{7}$$

The coefficient φ is a function of the fluid viscosity η and the geometry of the pore space. Dimensional considerations suggest that $\varphi = \varphi_0 \eta$, where φ_0 is a dimensionless shape factor.

Equation 7 has been written down by analogy with the classical fluid mechanics (Landau and Lifschitz 1959). The stress σ^{f} acts on saturated porous medium, whereas the flow is governed by Darcy's law. Therefore, this is different from the shear stress in the Brinkman model (Brinkman 1947). We do not know any experimental data on stress σ^{f}. The asymptotic analysis below shows that σ^{f} enters only higher-order terms and can be ignored in the low-frequency range.

2.5 Momentum Balance in a Planar Wave

From the previous sections, the total stress, σ^{t}, is the sum of all three stresses components defined in Eqs. 2, 3, and 7: $\sigma^{\mathrm{t}} = \sigma^{\mathrm{s}} + \sigma^{\mathrm{p}} + \sigma^{\mathrm{f}}$. Let us denote by ϱ_{g} the density of the solid constituent, so that the bulk density is equal to $\varrho_{\mathrm{b}} = \phi\varrho_{\mathrm{f}} + (1-\phi)\varrho_{\mathrm{g}}$. The linearized momentum balance equation has the following form

$$\varrho_{\mathrm{b}} \frac{\partial^2 \mathbf{u}}{\partial t^2} + \varrho_{\mathrm{f}} \frac{\partial \mathbf{W}}{\partial t} = \nabla \cdot \sigma^{\mathrm{t}} \tag{8}$$

For a planar wave propagating in direction x, all the derivatives with respect to y and z vanish. A substitution of equations 2, 3, and 7 reduces Eq. 8 to

$$\begin{aligned} \varrho_{\mathrm{b}} \frac{\partial^2 u_x}{\partial t^2} + \varrho_{\mathrm{f}} \frac{\partial W_x}{\partial t} &= M \frac{\partial^2 u_x}{\partial x^2} - \alpha \frac{\partial p}{\partial x} \\ \varrho_{\mathrm{b}} \frac{\partial^2 u_y}{\partial t^2} + \varrho_{\mathrm{f}} \frac{\partial W_y}{\partial t} &= \mu \frac{\partial^2 u_y}{\partial x^2} - \varphi \frac{\partial^2 W_y}{\partial x^2} \\ \varrho_{\mathrm{b}} \frac{\partial^2 u_z}{\partial t^2} + \varrho_{\mathrm{f}} \frac{\partial W_z}{\partial t} &= \mu \frac{\partial^2 u_z}{\partial x^2} - \varphi \frac{\partial^2 W_z}{\partial x^2} \end{aligned} \tag{9}$$

where $M = K + \frac{4}{3}\mu$.

2.6 Mass Balance

The variation of the fluid mass in an elementary volume due to the deformation of the skeleton and fluid compression equals the total mass flux through the boundary of the volume. Assuming adiabatic linear fluid compressibility and retaining only the first-order terms, one obtains

$$\beta_{\mathrm{f}}\phi\frac{\partial p}{\partial t}+\frac{\partial \phi}{\partial t}+\nabla\cdot\mathbf{W}+\phi\nabla\cdot\frac{\partial \mathbf{u}}{\partial t}=0 \tag{10}$$

Here β_{f} is the coefficient of adiabatic compressibility of the fluid: $\frac{\mathrm{d}\varrho_{\mathrm{f}}}{\varrho_{\mathrm{f}}}=\beta_{\mathrm{f}}\mathrm{d}p$. The linearized mass balance equation for the skeleton is:

$$(1-\phi)\frac{1}{\varrho_{\mathrm{g}}}\frac{\partial \varrho_{\mathrm{g}}}{\partial t}-\frac{\partial \phi}{\partial t}=-(1-\phi)\nabla\cdot\frac{\partial \mathbf{u}}{\partial t} \tag{11}$$

We assume that the compression of the grains is determined by the component of the skeleton stress coming from the volumetric strain (described by the term $K\nabla\cdot\mathbf{u}$ in Eq. 2) and the fluid pressure variations. In a linearized form, one obtains:

$$\frac{1}{\varrho_{\mathrm{g}}}\,\mathrm{d}\varrho_{\mathrm{g}}=-\frac{1}{K_{\mathrm{sg}}}K\nabla\cdot\mathbf{u}+\frac{1}{K_{\mathrm{fg}}}\mathrm{d}p \tag{12}$$

Here K_{sg} and K_{fg} are the elastic moduli quantifying the compression of the grains by the volumetric strain of the skeleton and the fluid pressure variations, respectively. Thus, in terms of time derivatives, one obtains

$$\frac{1}{\varrho_{\mathrm{g}}}\frac{\partial \varrho_{\mathrm{g}}}{\partial t}=-\frac{K}{K_{\mathrm{sg}}}\nabla\cdot\frac{\partial \mathbf{u}}{\partial t}+\frac{1}{K_{\mathrm{fg}}}\frac{\partial p}{\partial t} \tag{13}$$

The time derivative of the porosity can be eliminated from Eqs. 10 and 11. After gathering similar terms, one obtains:

$$\frac{\gamma_\beta}{K}\frac{\partial p}{\partial t}+\gamma_K\nabla\cdot\frac{\partial \mathbf{u}}{\partial t}+\nabla\cdot\mathbf{W}=0 \tag{14}$$

where the dimensionless coefficients γ_K and γ_β are defined by

$$\gamma_\beta=K\left(\beta_{\mathrm{f}}\phi+\frac{1-\phi}{K_{\mathrm{fg}}}\right)\quad\text{and}\quad\gamma_K=1-\frac{(1-\phi)K}{K_{\mathrm{sg}}} \tag{15}$$

2.7 Some Remarks

The skeleton is less stiff than the grain material: $K\le K_{\mathrm{v}}$. Thus, $\phi\le\gamma_K\le 1$. At vanishing porosity, $\phi\to 0$, the skeleton strength approaches that of the grain material, $K/K_{\mathrm{sg}}\to 1$. Therefore, if the transition to the zero porosity is smooth, which according to Hashin (1964) and Budiansky (1965) holds true for a variety of heterogeneous media, then

$$\gamma_K\sim\phi\quad\text{as }\phi\to 0 \tag{16}$$

Equation 15 implies that $\gamma_\beta\ge K\beta_{\mathrm{f}}\phi$. The compressibility of the fluid, β_{f}, is independent of the porosity, whereas the bulk modulus of the skeleton, K, converges to that of the grain material as $\phi\to 0$. Thus, the product $K\beta_{\mathrm{f}}$ does not vanish and Eq. 16 implies that

$$\gamma_\beta\gg\phi^2\sim\gamma_K^2\quad\text{as }\phi\to 0 \tag{17}$$

This estimate will be used below.

To compare the introduced coefficients to those of Biot and Willis (1957), one can introduce a fluid displacement vector, $\mathbf{w}$, as the integral of the Darcy velocity:

$$\mathbf{W} = \frac{\mathrm{d}}{\mathrm{d}t}\mathbf{w} \tag{18}$$

Integration of Eq. 14 with respect to t yields

$$p = -\frac{K\gamma_K}{\gamma_\beta}\nabla\cdot\mathbf{u} - \frac{K}{\gamma_\beta}\nabla\cdot\mathbf{w} \tag{19}$$

The divergence in the last term, $\nabla\cdot\mathbf{w}$, is equal to the fluid content parameter (Biot and Willis 1957; Berryman 1981; Detournay and Chang 1993). A comparison of the last equation to equation (Biot and Willis 1957, (31)) shows that

$$\alpha_{\mathrm{BW}} = \gamma_K, \quad \text{and } M_{\mathrm{BW}} = \frac{K}{\gamma_\beta} \tag{20}$$

where the subscript $_{\mathrm{BW}}$ refers to the Biot–Willis coefficients in the notations of Biot and Willis (1957), and γ_K and γ_β are defined in Eq. 15. Equation 32 below shows that in fact $\gamma_K = \alpha$, where α is the geometric factor in Eqs. 3 and 9.

3 Asymptotic Harmonic Wave Solution

Let us seek a harmonic planar-wave solution to the obtained system of equations. That is, put

$$\mathbf{u} = \mathbf{U}_0 e^{i(\omega t - k_x x)},\ \mathbf{W} = \mathbf{W}_0 e^{i(\omega t - k_x x)}, \quad \text{and } p = p_0 e^{i(\omega t - k_x x)} \tag{21}$$

Here k_x denotes the x-component of the complex-valued wave vector: $\mathbf{k} = (k_x, 0, 0)$. A substitution of Eq. 21 into Eqs. 9, 6, and 10 yields

$$\begin{aligned}
-\omega^2\varrho_{\mathrm{b}}U_{0x} + i\omega\varrho_{\mathrm{f}}W_{0x} &= -Mk_x^2U_{0x} + ik_x\alpha p_0\\
-\omega^2\varrho_{\mathrm{b}}U_{0y} + i\varrho_{\mathrm{f}}\omega W_{0y} &= -\mu k_x^2U_{0y} + \varphi k_x^2W_{0y}\\
-\omega^2\varrho_{\mathrm{b}}U_{0z} + i\varrho_{\mathrm{f}}\omega W_{0z} &= -\mu k_x^2U_{0z} + \varphi k_x^2W_{0z}\\
W_{0x} + i\omega\tau W_{0x} &= \frac{\kappa}{\eta}\left(ik_x p_0 + \omega^2\varrho_{\mathrm{f}}U_{0x}\right)\\
W_{0y} + i\omega\tau W_{0y} &= \frac{\kappa}{\eta}\omega^2\varrho_{\mathrm{f}}U_{0y}\\
W_{0z} + i\omega\tau W_{0z} &= \frac{\kappa}{\eta}\omega^2\varrho_{\mathrm{f}}U_{0z}\\
i\omega\frac{\gamma_\beta}{M}p_0 + \gamma_K k_x\omega U_{0x} &= ik_xW_{0x}
\end{aligned} \tag{22}$$

Like in the classical case, the compression and shear waves decouple and each component of the solution can be calculated separately.

3.1 Compression Wave

The system of compression wave equations consists of only those equations (22), which involve the x-components of the skeleton displacement and the Darcy velocity:

$$\begin{aligned} -\omega^2\varrho_{\mathrm{b}}U_{0x} + i\varrho_{\mathrm{f}}\omega W_{0x} &= -Mk_x^2U_{0x} + ik_x\alpha p_0 \\ W_{0x} + i\omega\tau W_{0x} &= \frac{\kappa}{\eta}\left(ik_x p_0 + \omega^2\varrho_{\mathrm{f}}U_{0x}\right) \\ i\omega\frac{\gamma_\beta}{M}p_0 + \gamma_K k_x\omega U_{0x} &= ik_x W_{0x} \end{aligned} \tag{23}$$

For low frequencies, formula $\varepsilon = i\lambda\omega$ defines a dimensionless small parameter, where the quantity $\lambda = \varrho_{\mathrm{f}}\frac{\kappa}{\eta}$ can be called kinematic reservoir fluid mobility. Let us define unknown dimensionless parameters:

$$\zeta = \frac{v^2}{v_{\mathrm{f}}^2}, \quad \xi = -i\frac{p_0}{k_x M U_{0x}}, \quad \text{and } \chi = i\frac{W_{0x}}{\omega U_{0x}} \tag{24}$$

Here $v^2 = \frac{\omega^2}{k_x^2}$ and $v_{\mathrm{f}}^2 = \frac{M}{\varrho_{\mathrm{f}}}$. Then, the system of equations (23) takes on the form:

$$\gamma_\varrho\zeta - \zeta\chi - \alpha\xi = 1 \tag{25}$$

$$\varepsilon(\zeta - \vartheta\zeta\chi - \xi) - \zeta\chi = 0 \tag{26}$$

$$\gamma_\beta\xi + \chi = \gamma_K \tag{27}$$

where $\gamma_\varrho = \frac{\varrho_{\mathrm{b}}}{\varrho_{\mathrm{f}}}$ and $\vartheta = \frac{\tau}{\lambda}$. We seek a solution to the system (25)–(27) in the form of power series in ε:

$$\begin{aligned} \zeta &= \zeta_0 + \zeta_1\varepsilon + \zeta_2\varepsilon^2 + \cdots, \quad \chi = \chi_0 + \chi_1\varepsilon + \chi_2\varepsilon^2 + \cdots, \\ \xi &= \xi_0 + \xi_1\varepsilon + \xi_2\varepsilon^2 + \cdots \end{aligned} \tag{28}$$

where "$\cdots$" denotes the higher-order terms.

At $\varepsilon = 0$, Eq. 26 implies $\zeta_0\chi_0 = 0$. One obtains two zero-order solutions:

$$\begin{aligned} \zeta_0^{\mathrm{S}} &= 0 & \zeta_0^{\mathrm{F}} &= \tfrac{\alpha\gamma_K + \gamma_\beta}{\gamma_\beta\gamma_\varrho} \\ \xi_0^{\mathrm{S}} &= -\tfrac{1}{\alpha} & \xi_0^{\mathrm{F}} &= \tfrac{\gamma_K}{\gamma_\beta} \\ \chi_0^{\mathrm{S}} &= \gamma_K + \tfrac{\gamma_\beta}{\alpha} & \chi_0^{\mathrm{F}} &= 0 \end{aligned} \tag{29}$$

The superscripts $^{\mathrm{S}}$ and $^{\mathrm{F}}$ stand for the slow and fast waves. To determine the first-order terms, one has to solve the following system of equations:

$$\begin{aligned} \gamma_\varrho\zeta_1 - \zeta_0\chi_1 - \chi_0\zeta_1 - \alpha\xi_1 &= 0 \\ \zeta_0\chi_1 + \chi_0\zeta_1 &= \zeta_0 - \vartheta\chi_0\zeta_0 - \xi_0 \\ \gamma_\beta\xi_1 + \chi_1 &= 0 \end{aligned} \tag{30}$$

Note that ϑ is the only dimensionless parameter depending on the parameter τ in the dynamic Darcy's law, Eq. 6. Since $\chi_0\zeta_0 = 0$, the term involving ϑ vanishes both for the slow-wave and the fast-wave solutions. Consequently, the classical steady-state Darcy's law formulation is sufficient for the first-order asymptotic analysis.

The solution to the system of equations (31) is:

$$\begin{array}{ll} \zeta_1^{\mathrm{S}} = \frac{1}{\alpha\gamma_K+\gamma_\beta} & \zeta_1^{\mathrm{F}} = \frac{\zeta_0^{\mathrm{F}}-\frac{\alpha}{\gamma_\beta}}{\gamma_\varrho \zeta_0^{\mathrm{F}}}\left(\zeta_0^{\mathrm{F}}-\xi_0^{\mathrm{F}}\right) \\ \xi_1^{\mathrm{S}} = \frac{1}{\alpha}\frac{\gamma_\varrho}{\alpha\gamma_K+\gamma_\beta}-\frac{1}{\alpha} & \xi_1^{\mathrm{F}} = \frac{\gamma_K\gamma_\varrho}{(\alpha\gamma_K+\gamma_\beta)\gamma_\beta}-\frac{1}{\gamma_\beta} \\ \chi_1^{\mathrm{S}} = -\frac{1}{\alpha}\frac{\gamma_\varrho\gamma_\beta}{\alpha\gamma_K+\gamma_\beta}+\frac{\gamma_\beta}{\alpha} & \chi_1^{\mathrm{F}} = 1-\frac{\gamma_K\gamma_\varrho}{\alpha\gamma_K+\gamma_\beta} \end{array} \tag{31}$$

From equations (29), $\zeta_0^{\mathrm{F}} > 0$. The solution is physically sensible only if ζ_1^{F} is a positive quantity. This requirement is fulfilled for an arbitrary ζ_0^{F} only if $\frac{\alpha}{\gamma_\beta} = \xi_0^{\mathrm{F}}$. Substituting the expression for ξ_0^{F} from Eq. 29, one obtains:

$$\alpha = \gamma_K = 1 - \frac{(1-\phi)K}{K_{\mathrm{sg}}} \tag{32}$$

Finally, Eqs. 29 and 31 can be rewritten in the form:

$$\begin{array}{ll} \zeta_0^{\mathrm{S}} = 0 & \zeta_0^{\mathrm{F}} = \frac{{\gamma_K}^2+\gamma_\beta}{\gamma_\beta\gamma_\varrho} \\ \xi_0^{\mathrm{S}} = -\frac{1}{\gamma_K} & \xi_0^{\mathrm{F}} = \frac{\gamma_K}{\gamma_\beta} \\ \chi_0^{\mathrm{S}} = \frac{{\gamma_K}^2+\gamma_\beta}{\gamma_K} & \chi_0^{\mathrm{F}} = 0 \end{array} \tag{33}$$

and

$$\begin{array}{ll} \zeta_1^{\mathrm{S}} = \frac{1}{{\gamma_K}^2+\gamma_\beta} & \zeta_1^{\mathrm{F}} = \frac{1}{\gamma_\beta({\gamma_K}^2+\gamma_\beta)}\left(\frac{{\gamma_K}^2+\gamma_\beta}{\gamma_\varrho}-\gamma_K\right)^2 \\ \xi_1^{\mathrm{S}} = \frac{1}{\gamma_K}\frac{\gamma_\varrho}{{\gamma_K}^2+\gamma_\beta}-\frac{1}{\gamma_K} & \xi_1^{\mathrm{F}} = \frac{\gamma_K\gamma_\varrho}{({\gamma_K}^2+\gamma_\beta)\gamma_\beta}-\frac{1}{\gamma_\beta} \\ \chi_1^{\mathrm{S}} = -\frac{1}{\gamma_K}\frac{\gamma_\varrho\gamma_\beta}{{\gamma_K}^2+\gamma_\beta}+\frac{\gamma_\beta}{\gamma_K} & \chi_1^{\mathrm{F}} = 1-\frac{\gamma_K\gamma_\varrho}{{\gamma_K}^2+\gamma_\beta} \end{array} \tag{34}$$

From the leftmost equation (24), $k_x^2 = \frac{\varrho_{\mathrm{f}}}{M\zeta}\omega^2$. Hence, for the fast wave,

$$k_x^{\mathrm{F}} = \frac{\omega}{v_{\mathrm{b}}}\sqrt{\frac{\gamma_\beta}{\gamma_\beta+{\gamma_K}^2}}\left(1-\frac{\zeta_1^{\mathrm{F}}}{2\zeta_0^{\mathrm{F}}}\varepsilon+O(|\varepsilon|^2)\right) \tag{35}$$

where $v_{\mathrm{b}}^2 = \frac{M}{\varrho_{\mathrm{b}}}$. For the slow wave,

$$k_x^{\mathrm{S}} = \frac{\omega}{v_{\mathrm{f}}}\sqrt{\frac{{\gamma_K}^2+\gamma_\beta}{2\,|\varepsilon|}}(1-i)\,(1+O(|\varepsilon|)) \tag{36}$$

In the last equation, the branch of the square root has been selected to guarantee that $\mathrm{Im}(k_x^{\mathrm{S}}) < 0$, that is, $\sqrt{\varepsilon} = \frac{1+i}{\sqrt{2}}\sqrt{|\varepsilon|} = \sqrt{|\varepsilon|}e^{i\frac{\pi}{4}}$. Equations 35 and 36 can be rearranged into the from:

$$k_x^{\mathrm{F}} = \omega\left(k_0^{\mathrm{F}}+k_1^{\mathrm{F}}\varepsilon+O(|\varepsilon|^2)\right) \tag{37}$$

$$k_x^{\mathrm{S}} = \omega\left(k_0^{\mathrm{S}}\frac{1}{\sqrt{\varepsilon}}+k_1^{\mathrm{S}}\sqrt{\varepsilon}+O(|\varepsilon|^{3/2})\right) \tag{38}$$

where

$$k_0^{\mathrm{F}} = \frac{1}{v_{\mathrm{b}}}\sqrt{\frac{\gamma_\beta}{\gamma_\beta+{\gamma_K}^2}} \quad \text{and} \quad k_0^{\mathrm{S}} = \frac{1}{v_{\mathrm{f}}}\sqrt{\gamma_\beta+{\gamma_K}^2} \tag{39}$$

Note that the estimate in Eq. 17 implies $k_0^{\mathrm{F}} \approx \frac{1}{v_{\mathrm{b}}}$ as $\phi \to 0$. The velocities and attenuation factors for the fast and slow waves are

$$V^{\mathrm{F}} = v_{\mathrm{b}} \sqrt{1 + \frac{{\gamma_K}^2}{\gamma_\beta}} \left(1 + O(|\varepsilon|^2)\right) \tag{40}$$

$$V^{\mathrm{S}} = v_{\mathrm{F}} \sqrt{\frac{2\,|\varepsilon|}{\gamma_\beta + {\gamma_K}^2}} \left(1 + O(|\varepsilon|)\right) \tag{41}$$

$$a^{\mathrm{F}} = \frac{\omega}{v_{\mathrm{b}}} \sqrt{\frac{\gamma_\beta}{\gamma_\beta + {\gamma_K}^2}} \frac{\zeta_1^{\mathrm{F}}}{2\zeta_0^{\mathrm{F}}}\ |\varepsilon|\ \left(1 + O(|\varepsilon|^2)\right) \tag{42}$$

$$a^{\mathrm{S}} = \frac{\omega}{v_{\mathrm{f}}} \sqrt{\frac{\gamma_\beta + {\gamma_K}^2}{2\,|\varepsilon|}} \left(1 + O(|\varepsilon|)\right) \tag{43}$$

By the definition of ε, the angular frequency ω is present both in the numerator and the denominator in the last equation. It is useful to rewrite it in an alternative from

$$a^{\mathrm{S}} = \frac{\eta}{\kappa} \sqrt{\frac{\gamma_\beta + \gamma_K^2}{2M\varrho_{\mathrm{f}}}} \sqrt{|\varepsilon|} \tag{44}$$

Clearly, $V^{\mathrm{F}} \gg V^{\mathrm{S}} = O\left(\sqrt{|\varepsilon|}\right)$ and $a^{\mathrm{F}} \ll a^{\mathrm{S}}$ as $\varepsilon \to 0$. Equation 16 also implies that, for $\phi \to 0$, the fast compressive wave velocity approaches the velocity of sound in a medium whose density is equal to the density of the grains and elastic moduli are those of the drained skeleton. Finally, the power series asymptotic expressions for the Darcy velocity and the fluid pressure have the following forms:

$$W_{0x}^{\mathrm{F}} = -i\omega\varepsilon \left(\chi_1^{\mathrm{F}} + O(|\varepsilon|)\right) U_{0x}^{\mathrm{F}} \tag{45}$$

$$W_{0x}^{\mathrm{S}} = -i\omega \frac{\gamma_\beta + {\gamma_K}^2}{\gamma_K} \left(1 + \frac{\chi_1^{\mathrm{S}}}{\chi_0^{\mathrm{S}}}\varepsilon + O(|\varepsilon|^2)\right) U_{0x}^{\mathrm{S}} \tag{46}$$

$$p_0^{\mathrm{F}} = \omega \left[k_0^{\mathrm{F}} + (k_1^{\mathrm{F}}\xi_0^{\mathrm{F}} + k_0^{\mathrm{F}}\xi_1^{\mathrm{F}})\varepsilon + O(|\varepsilon|^2)\right] M U_{0x}^{\mathrm{F}} \tag{47}$$

$$p_0^{\mathrm{S}} = \frac{\omega}{\sqrt{|\varepsilon|}} \left[k_0^{\mathrm{S}} + (k_1^{\mathrm{S}}\xi_0^{\mathrm{S}} + k_0^{\mathrm{S}}\xi_1^{\mathrm{S}})\varepsilon + O(|\varepsilon|^2)\right] M U_{0x}^{\mathrm{S}} \tag{48}$$

3.2 Shear Wave

The shear waves in the directions y and z are analogous to each other; so we consider in detail only the shear wave in the direction y. Since shear deformation includes zero volumetric strain, the mass balance equation (14) is an identity. Thus, the following system of two equations needs to be solved:

$$\begin{aligned} -\omega^2 \varrho_{\mathrm{b}} U_{0y} + i\varrho_{\mathrm{f}}\omega W_{0y} &= \mu {k_x}^2 U_{0y} - \chi {k_x}^2 W_{0y} \\ W_{0y} + i\omega\tau W_{0y} &= \frac{\kappa}{\eta}\omega^2 \varrho_{\mathrm{f}} U_{0y} \end{aligned} \tag{49}$$

A convenient set of dimensionless variables is provided by the first and last equations (24), where the x-components are replaced with the respective y-components. The system of equations (49) transforms into the following:

$$\begin{aligned} \gamma_\varrho \zeta - \zeta\chi + \varepsilon \frac{\chi\eta}{\mu\varrho_{\mathrm{f}}\kappa}\chi &= 1 \\ \chi + \varepsilon\vartheta\chi &= \varepsilon \end{aligned} \tag{50}$$

which is equivalent to Eqs. 25–26 if one puts $\xi = 0$ and replaces M with μ. The solution to the system (50) is:

$$\zeta = \frac{1 - \frac{\varepsilon^2}{1+\varepsilon\vartheta}\frac{\chi\eta}{\mu\varrho_{\mathrm{f}}\kappa}}{\gamma_\varrho - \frac{\varepsilon}{1+\varepsilon\vartheta}} \quad \text{and} \quad \chi = \frac{\varepsilon}{1+\varepsilon\vartheta} \tag{51}$$

In the form of a power series in ε, this solution takes on the form:

$$\zeta = \frac{1}{\gamma_\varrho} + \frac{1}{{\gamma_\varrho}^2}\varepsilon + O(|\varepsilon|^2), \quad \chi = \varepsilon(1 - \vartheta\varepsilon + O(|\varepsilon|^2)) \tag{52}$$

Note that the shear wave solution has no slow-wave component.
Returning to the physical quantities, one obtains

$$k_x^{\mathrm{H}} = \sqrt{\frac{\varrho_{\mathrm{b}}}{\mu}}\omega\left(1 - \frac{1}{2\gamma_\varrho}\varepsilon + O\left(|\varepsilon|^2\right)\right) \tag{53}$$

where the superscript $^{\mathrm{H}}$ denotes a shear wave. Thus, $k_0^{\mathrm{H}} = \sqrt{\varrho_{\mathrm{b}}/\mu}$ in the power-series expansion $k^{\mathrm{H}} = \omega\left(k_0^{\mathrm{H}} + k_1^{\mathrm{H}}\varepsilon + O(|\varepsilon|^2)\right)$. For the attenuation factor, a^{H}, and the velocity, V^{H}, one obtains

$$a^{\mathrm{H}} = \sqrt{\frac{\varrho_{\mathrm{b}}}{\mu}}\frac{|\varepsilon|}{2\gamma_\varrho}\omega\left(1 + O\left(|\varepsilon|^2\right)\right), \quad V^{\mathrm{H}} = \sqrt{\frac{\mu}{\varrho_{\mathrm{b}}}}\left(1 + O\left(|\varepsilon|^2\right)\right) \tag{54}$$

3.3 Further Remarks

Let us demonstrate that the equations above are consistent with the classical theory of poroelasticity.

3.3.1 Dynamic Darcy's Law and Flow-Imposed Shear Stress

For an oscillatory fluid flow in a porous medium, Johnson et al. (1987) have obtained a modification of Darcy's law, in which the coefficient of permeability depends on the frequency of the oscillations:

$$W = -\frac{\widetilde{\kappa}(\omega)}{\eta}\nabla P \tag{55}$$

At the zero frequency limit, the frequency-dependent coefficient of permeability must be equal to the classical Darcy permeability: $\widetilde{\kappa}(0) = \kappa$. Therefore, one can write:

$$A(i\omega)\widetilde{\kappa}(\omega) = \kappa \text{ with } A(0) = 1 \tag{56}$$

Using Taylor expansion, $A(i\omega) = 1 + A'(0)i\omega + \cdots$, and truncating the higher-order terms, one obtains from Eq. 55:

$$W + A'(0)i\omega W = -\frac{\kappa}{\eta}\nabla P \tag{57}$$

The last equation is equivalent to Eq. 6 for $\tau = A'(0)$.

Equations 29, 31, and 52 imply that both, the dynamic term in the dynamic Darcy's law, Eq. 6, and the flow-induced shear stress, affect only the power series terms of the order of $O(|\varepsilon|^2)$ or higher. Thus, the classical steady-state formulation of Darcy's law is sufficient for the first-order asymptotic approximation of the compression wave solution.

3.3.2 Elastic Moduli

The compressibility of the fluid and the moduli of drained skeleton can be determined in laboratory tests. The other two moduli introduces in Eq. 12 also can be determined experimentally. For the first test, one can change the pore pressure by injecting or withdrawing fluid while maintaining the total stress constant. From the fluid compressibility and the variation of the fluid volume, one can evaluate the variation of the pore volume and, consequently, the variation of the total volume of the solid grains. Hence, from the known mass of the solid skeleton one obtains the variation of the average density of the grains. In an undrained uniaxial test, one also can measure the variation of the fluid pressure and the total volume of the saturated sample. Therefore, the variation of the average density of the grains can be calculated as well. Thus, knowing K from independent measurements, one obtains a system of two equations, which can be solved for the moduli K_{sg} and K_{fg}.

3.3.3 Biot's Equations

Equations 32 and 20 show that the coefficient α introduced in Sect. 3 and the Biot–Willis coefficients α are the same. Further on, Eq. 19 makes possible to eliminate the fluid pressure p from the first Eqs. 9 and 6. Thus, using the notation (18), one obtains:

$$\varrho_{\mathrm{b}}\frac{\partial^2 u_x}{\partial t^2}+\varrho_{\mathrm{f}}\frac{\partial^2 w_x}{\partial t^2}=\left[K\left(1+\frac{{\gamma_K}^2}{\gamma_\beta}\right)+\frac{4}{3}\mu\right]\frac{\partial^2 u_x}{\partial x^2}+\frac{K\gamma_K}{\gamma_\beta}\frac{\partial^2 w}{\partial x^2} \tag{58}$$

$$\varrho_{\mathrm{f}}\frac{\partial^2 u_x}{\partial t^2}+\tau\frac{\eta}{\kappa}\frac{\partial^2 w_x}{\partial t^2}=\frac{K\gamma_K}{\gamma_\beta}\frac{\partial^2 u_x}{\partial x^2}+\frac{K}{\gamma_\beta}\frac{\partial^2 w}{\partial x^2}-\frac{\eta}{\kappa}\frac{\partial w_x}{\partial t} \tag{59}$$

The last system of equations is equivalent to Biot's equations (Biot 1962) with the following mapping rule:

$$\begin{array}{ll} A\leftrightarrow K\left(1+\frac{{\gamma_K}^2}{\gamma_\beta}\right)+\frac{4}{3}\mu & M_{11}\leftrightarrow\frac{K\gamma_K}{\gamma_\beta} \\ M\leftrightarrow\frac{K}{\gamma_\beta} & m\leftrightarrow\tau\frac{\eta}{\kappa} \end{array} \tag{60}$$

The notations and the parameters on the left-hand sides of these relationships are from Biot (1962).

In some works, parameter m is associated with the formation resistivity factor (Brown 1980). In any case, parameter τ does not affect the zero- and first-order terms in the asymptotic analysis above.

3.3.4 Nikolaevskii's Model

Nikolaevskii, see Nikolaevskii et al. (1970) and Nikolaevskii (1996), has developed a general model of poroelasticity based on mass, momentum, and energy balance. Besides purely mechanical deformation, his model accounts for the impact of heating on stress and deformation. For isothermal creeping flow, the model developed here is consistent with the Nikolaevskii model. The mass balance equations (10) and (11) are equivalent to equations (Nikolaevskii 1996, (2.1)–(2.2)). We neglect the gravity; therefore, the momentum balance equation for the bulk medium, Eq. 8, is equivalent to the linearized equation (Nikolaevskii 1996, (2.3)). Let us demonstrate that Eq. 6 is equivalent to linearized Nikolaevskii's equation of momentum balance for the fluid in an isotropic medium. In our notations, a linearization of equation (Nikolaevskii 1996, (2.5)) yields:

$$\frac{\partial}{\partial t}\left(\varrho_{\mathrm{f}}\mathbf{W}+\varrho_{\mathrm{f}}\phi\frac{\partial\mathbf{u}}{\partial t}\right)=-\phi\nabla p+\mathbf{R} \tag{61}$$

where $\mathbf{R}$ is called the viscose resistance to the fluid flow (Nikolaevskii 1996). In an isotropic medium, linearized equations (Nikolaevskii 1996, (2.31), (2.65)) imply the following expression for $\mathbf{R}$:

$$\mathbf{R}=-\phi^2\frac{\eta}{\kappa}\left(\frac{1}{\phi}\mathbf{W}\right) \tag{62}$$

Since the Darcy velocity and skeleton displacement are small, a substitution of Eq. 62 into (61), after canceling ϕ, gives:

$$\mathbf{W}+\frac{\varrho_{\mathrm{f}}\kappa}{\eta\phi}\frac{\partial\mathbf{W}}{\partial t}=-\frac{\kappa}{\eta}\left(\nabla p+\varrho_{\mathrm{f}}\frac{\partial^2\mathbf{u}}{\partial t^2}\right) \tag{63}$$

The latter equation is identical to Eq. 6 if one puts $\tau_*=0$ and $\tau=\frac{\varrho_{\mathrm{f}}\kappa}{\eta\phi}$.

3.3.5 Gassmann's Model

The two elastic moduli, K_{sg} and K_{fg}, defined in Eq. 12 relate the grain volumetric strain to the skeleton stress and fluid pressure, respectively. If the relationships

$$K_{\mathrm{sg}}=\frac{K_{\mathrm{g}}}{1-\phi}\quad\text{and}\quad K_{\mathrm{fg}}=\frac{K_{\mathrm{g}}}{1-\frac{K}{K_{\mathrm{g}}}} \tag{64}$$

hold true, then the expression $K\left(1+\frac{\gamma_K{}^2}{\gamma_\beta}\right)$ yields Gassmann's bulk modulus (Gassmann 1951; Pelissier et al. 2007).

3.4 Vanishing Attenuation

For some combinations of parameters, the coefficient ζ_1^{F} defined in Eq. 31 can vanish. In such a case, the first-order approximation of the fast wave attenuation, Eq. 42, is equal to zero. For example, $\zeta_1^{\mathrm{F}}=0$ if $\gamma_K=\sqrt{\gamma_\beta}$ and $\gamma_\varrho=2\gamma_K$ simultaneously.

4 Normal Reflection of a Compression Wave

Let two poroelastic media labeled by the superscripts ^{1} and ^{2} have a permeable plane interface at $x=0$. A fast or slow incident wave generates four waves: fast and slow reflected waves, and fast and slow transmitted waves, Fig. 3. Let us consider fast and slow incident waves separately.

4.1 Fast Incident Wave

A fast incident wave arriving from the half-space $x<0$ generates four waves: the fast and slow reflected waves and the fast and slow transmitted waves. Thus, in the medium 1, the displacement can be characterized as

$$u_1(t,x)=U_0e^{i(\omega t-k^{1\mathrm{F}}x)}+R^{\mathrm{FF}}U_0e^{i(\omega t+k^{1\mathrm{F}}x)}+R^{\mathrm{FS}}U_0e^{i(\omega t+k^{1\mathrm{S}}x)} \tag{65}$$

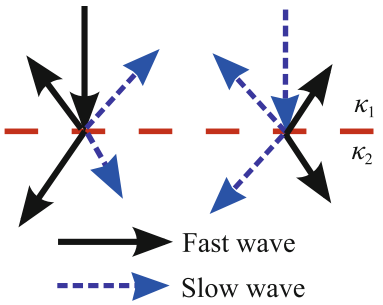

Fig. 3 Fast or slow incident normal wave generates four waves at a planar interface: a reflected and transmitted fast wave, and a reflected and transmitted slow wave

whereas in Medium 2, the skeleton displacement is

$$u_2(t,x) = T^{\mathrm{FF}} U_0 e^{i(\omega t - k^{2\mathrm{F}} x)} + T^{\mathrm{FS}} U_0 e^{i(\omega t - k^{2\mathrm{S}} x)} \tag{66}$$

Here R^{FF}, R^{FS}, T^{FF}, and T^{FS} are the respective reflection and transmission coefficients. The first letter in the superscript denotes the fast incident wave, whereas the second one denotes the fast or slow reflected or transmitted wave.

The mass and momentum balance imply that the skeleton displacement, the Darcy velocity of the fluid, the total stress, and the fluid pressure must be continuous at the interface. Using notations (24), one obtains the following system of boundary conditions

$$1 + R^{\mathrm{FF}} + R^{\mathrm{FS}} = T^{\mathrm{FF}} + T^{\mathrm{FS}} \tag{67}$$

$$\chi^{1\mathrm{F}}(1 + R^{\mathrm{FF}}) + \chi^{1\mathrm{S}} R^{\mathrm{FS}} = \chi^{2\mathrm{F}} T^{\mathrm{FF}} + \chi^{2\mathrm{S}} T^{\mathrm{FS}} \tag{68}$$

$$\begin{aligned} &M^1 k^{1\mathrm{F}}(1 + \gamma_K^1 \xi^{1\mathrm{F}})(1 - R^{\mathrm{FF}}) - M^1 k^{1\mathrm{S}}(1 + \gamma_K^1 \xi^{1\mathrm{S}}) R^{\mathrm{FS}} \\ &\quad = M^2 k^{2\mathrm{F}}(1 + \gamma_K^2 \xi^{2\mathrm{F}}) T^{\mathrm{FF}} + M^2 k^{2\mathrm{S}}(1 + \gamma_K^2 \xi^{2\mathrm{S}}) T^{\mathrm{FS}} \end{aligned} \tag{69}$$

$$\begin{aligned} &M^1 k^{1\mathrm{F}} \xi^{1\mathrm{F}}(1 - R^{\mathrm{FF}}) - M^1 k^{1\mathrm{S}} \xi^{1\mathrm{S}} R^{\mathrm{FS}} \\ &\quad = M^2 k^{2\mathrm{F}} \xi^{2\mathrm{F}} T^{\mathrm{FF}} + M^2 k^{2\mathrm{S}} \xi^{2\mathrm{S}} T^{\mathrm{FS}} \end{aligned} \tag{70}$$

To obtain asymptotic expressions for the reflection and transmission coefficients, we rewrite Eqs. 67–70 in an approximate form, retaining only the leading zero-order and the next after zero-order terms. For the first two equations, these terms are the constant ones and the ones which are linear in ε. For the last two equations, these terms are the constant ones and the ones proportional to $\sqrt{|\varepsilon|}$. One obtains:

$$1 + R^{\mathrm{FF}} + R^{\mathrm{FS}} = T^{\mathrm{FF}} + T^{\mathrm{FS}} \tag{71}$$

$$\varepsilon \chi_1^{1\mathrm{F}}(1 + R^{\mathrm{FF}}) + (\chi_0^{1\mathrm{S}} + \varepsilon \chi_1^{1\mathrm{S}}) R^{\mathrm{FS}} = \gamma_\kappa \varepsilon \chi_1^{2\mathrm{F}} T^{\mathrm{FF}} + (\chi_0^{2\mathrm{S}} + \chi_1^{2\mathrm{S}} \gamma_\kappa \varepsilon) T^{\mathrm{FS}} \tag{72}$$

$$\begin{aligned} &\sqrt{\varepsilon} M^1 k_0^{1\mathrm{F}} \left(1 + \gamma_K^1 \xi_0^{1\mathrm{F}}\right)(1 - R^{\mathrm{FF}}) - M^1 k_0^{1\mathrm{S}} \left(1 + \gamma_K^1 \xi_0^{1\mathrm{S}}\right) R^{\mathrm{FS}} \\ &\quad = \sqrt{\varepsilon} M^2 k_0^{2\mathrm{F}}(1 + \gamma_K^2 \xi_0^{2\mathrm{F}}) T^{\mathrm{FF}} + \frac{1}{\sqrt{\gamma_\kappa}} M^2 k_0^{2\mathrm{S}}(1 + \gamma_K^2 \xi_0^{2\mathrm{S}}) T^{\mathrm{FS}} \end{aligned} \tag{73}$$

$$\begin{aligned} &\sqrt{\varepsilon} M^1 k_0^{1\mathrm{F}} \xi_0^{1\mathrm{F}}(1 - R^{\mathrm{FF}}) - M^1 k_0^{1\mathrm{S}} \xi_0^{1\mathrm{S}} R^{\mathrm{FS}} \\ &\quad = \sqrt{\varepsilon} M^2 k_0^{2\mathrm{F}} \xi_0^{2\mathrm{F}} T^{\mathrm{FF}} + \frac{1}{\sqrt{\gamma_\kappa}} M^2 k_0^{2\mathrm{S}} \xi_0^{2\mathrm{S}} T^{\mathrm{FS}} \end{aligned} \tag{74}$$

Here

$$\gamma_\kappa = \frac{\varepsilon_2}{\varepsilon_1} = \frac{\kappa_2}{\kappa_1} = 1 + \frac{\kappa_2 - \kappa_1}{\kappa_1} \tag{75}$$

By virtue of equations (33),

$$1+\gamma_K^i \xi_0^{iF} = \frac{\gamma_\beta^i + \left(\gamma_K^i\right)^2}{\gamma_\beta^i} \quad \text{and} \quad 1+\gamma_K^i \xi_0^{1S} = 0, \quad i=1,2 \tag{76}$$

Thus, the slow-wave reflection and transmission terms vanish in Eq. 73. Taking into account Eq. 39, Eq. 73 reduces to

$$Z_1(1-R^{FF}) = Z_2 T^{FF} \tag{77}$$

where Z^i, $i=1,2$ are the modified acoustic impedances:

$$Z_i = \frac{M^i}{v_b^i}\sqrt{\frac{\gamma_\beta^i + (\gamma_K^i)^2}{\gamma_\beta^i}} \tag{78}$$

We seek asymptotic expressions for the transmission and reflection coefficients in the form

$$R = R_0 + R_1\sqrt{\varepsilon} + R_2\varepsilon + \cdots \quad \text{and } T = T_0 + T_1\sqrt{\varepsilon} + T_2\varepsilon + \cdots \tag{79}$$

We limit our calculations to the two leading terms only. Putting $\varepsilon = 0$ yields:

$$R_0^{FS} = T_0^{FS} = 0 \tag{80}$$

$$R_0^{FF} = \frac{Z_1 - Z_2}{Z_1 + Z_2} \text{ and } T_0^{FF} = \frac{2Z_1}{Z_1+Z_2} \tag{81}$$

Equations 73 and 74 imply

$$\frac{(\gamma_K^1)^2+\gamma_\beta^1}{\gamma_K^1} R_1^{FS} - \frac{(\gamma_K^2)^2+\gamma_\beta^2}{\gamma_K^2} T_1^{FS} = 0 \tag{82}$$

$$\begin{aligned} &\frac{M^1}{v_F^1}\frac{\sqrt{(\gamma_K^1)^2+\gamma_\beta^1}}{\gamma_K^1} R_1^{FS} + \frac{1}{\sqrt{\gamma_\kappa}}\frac{M^2}{v_F^2}\frac{\sqrt{(\gamma_K^2)^2+\gamma_\beta^2}}{\gamma_K^2} T_1^{FS} \\ &\quad = M^1 k_0^{1F}\xi_0^{1F}(1-R_0^{FF}) - M^2 k_0^{2F}\xi_0^{2F} T_0^{FF} \end{aligned} \tag{83}$$

The determinant of the linear system of Eqs. 82–83

$$\begin{aligned} D = &\frac{1}{\sqrt{\gamma_\kappa}}\frac{M^2}{v_F^2}\frac{(\gamma_K^1)^2+\gamma_\beta^1}{\gamma_K^1}\frac{\sqrt{(\gamma_K^2)^2+\gamma_\beta^2}}{\gamma_K^2} \\ &+\frac{M^1}{v_F^1}\frac{(\gamma_K^2)^2+\gamma_\beta^2}{\gamma_K^2}\frac{\sqrt{(\gamma_K^1)^2+\gamma_\beta^1}}{\gamma_K^1} \end{aligned} \tag{84}$$

is obviously positive: $D > 0$. Hence,

$$R_1^{FS} = \frac{A}{D}\frac{(\gamma_K^2)^2+\gamma_\beta^2}{\gamma_K^2} \quad \text{and } T_1^{FS} = \frac{A}{D}\frac{(\gamma_K^1)^2+\gamma_\beta^1}{\gamma_K^1} \tag{85}$$

where

$$A = \left[\frac{\gamma_K^1}{(\gamma_K^1)^2+\gamma_\beta^1} - \frac{\gamma_K^2}{(\gamma_K^2)^2+\gamma_\beta^2}\right]\frac{2\,Z_1 Z_2}{Z_1+Z_2} \tag{86}$$

For the next terms of the fast wave reflection and transmission coefficients, one obtains

$$R_1^{\mathrm{FF}} = \frac{Z_2(T_1^{\mathrm{FS}} - R_1^{\mathrm{FS}})}{Z_1 + Z_2} \quad \text{and } T_1^{\mathrm{FF}} = \frac{Z_1(R_1^{\mathrm{FS}} - T_1^{\mathrm{FS}})}{Z_1 + Z_2} \tag{87}$$

Finally,

$$R^{\mathrm{FF}} = \frac{Z_1^{\mathrm{F}} - Z_2^{\mathrm{F}}}{Z_1^{\mathrm{F}} + Z_2^{\mathrm{F}}} + R_1^{\mathrm{FF}} \frac{1+i}{\sqrt{2}} \sqrt{|\varepsilon|} + \cdots \tag{88}$$

$$T^{\mathrm{FF}} = 1 + \frac{Z_1^{\mathrm{F}} - Z_2^{\mathrm{F}}}{Z_1^{\mathrm{F}} + Z_2^{\mathrm{F}}} + T_1^{\mathrm{FF}} \frac{1+i}{\sqrt{2}} \sqrt{|\varepsilon|} + \cdots \tag{89}$$

4.2 Slow Incident Wave

A slow incident wave also generates four waves: the fast and slow reflected waves and the fast and slow transmitted waves. In the Medium 1, for a slow incident wave, one obtains

$$u_1(t,x) = U_0 e^{i(\omega t - k^{1\mathrm{S}} x)} + R^{\mathrm{SS}} U_0 e^{i(\omega t + k^{1\mathrm{S}} x)} + R^{\mathrm{SF}} U_0 e^{i(\omega t + k^{1\mathrm{F}} x)} \tag{90}$$

whereas in the Medium 2,

$$u_2(t,x) = T^{\mathrm{SF}} U_0 e^{i(\omega t - k^{2\mathrm{F}} x)} + T^{\mathrm{SS}} U_0 e^{i(\omega t - k^{2\mathrm{S}} x)} \tag{91}$$

Here R^{SS}, R^{SF}, T^{SF}, and T^{SS} are the respective reflection and transmission coefficients.

Equations 67–70 transform into

$$1 + R^{\mathrm{SS}} + R^{\mathrm{SF}} = T^{\mathrm{SF}} + T^{\mathrm{SS}} \tag{92}$$

$$\chi^{1\mathrm{S}}(1 + R^{\mathrm{SS}}) + \chi^{1\mathrm{F}} R^{\mathrm{SF}} = \chi^{2\mathrm{F}} T^{\mathrm{SF}} + \chi^{2\mathrm{S}} T^{\mathrm{SS}} \tag{93}$$

$$\begin{aligned} &-M^1 k^{1\mathrm{F}}(1 + \gamma_K^1 \xi^{1\mathrm{F}}) R^{\mathrm{SF}} + M^1 k^{1\mathrm{S}}(1 + \gamma_K^1 \xi^{1\mathrm{S}})(1 - R^{\mathrm{SS}}) \\ &\quad = M^2 k^{2\mathrm{F}}(1 + \gamma_K^2 \xi^{2\mathrm{F}}) T^{\mathrm{SF}} + M^2 k^{2\mathrm{S}}(1 + \gamma_K^2 \xi^{2\mathrm{S}}) T^{\mathrm{SS}} \end{aligned} \tag{94}$$

$$\begin{aligned} &-M^1 k^{1\mathrm{F}} \xi^{1\mathrm{F}} R^{\mathrm{SF}} + M^1 k^{1\mathrm{S}} \xi^{1\mathrm{S}}(1 - R^{\mathrm{SS}}) \\ &\quad = M^2 k^{2\mathrm{F}} \xi^{2\mathrm{F}} T^{\mathrm{SF}} + M^2 k^{2\mathrm{S}} \xi^{2\mathrm{S}} T^{\mathrm{SS}} \end{aligned} \tag{95}$$

After dropping the higher-order terms, one obtains

$$1 + R^{\mathrm{SS}} + R^{\mathrm{SF}} = T^{\mathrm{SF}} + T^{\mathrm{SS}} \tag{96}$$

$$\begin{aligned} &\varepsilon \chi_1^{1\mathrm{F}} R^{\mathrm{SF}} + (\chi_0^{1\mathrm{S}} + \varepsilon \chi_1^{1\mathrm{S}})(1 + R^{\mathrm{SS}}) \\ &\quad = \gamma_\kappa \varepsilon \chi_1^{2\mathrm{F}} T^{\mathrm{SF}} (\chi_0^{2\mathrm{S}} + \chi_1^{2\mathrm{S}} \gamma_\kappa \varepsilon) T^{\mathrm{SS}} \end{aligned} \tag{97}$$

$$-Z_1 R^{\mathrm{SF}} = Z_2 T^{\mathrm{SF}} \tag{98}$$

$$\begin{aligned} &-\sqrt{\varepsilon} M^1 k_0^{1\mathrm{F}} \xi_0^{1\mathrm{F}} R^{\mathrm{SF}} + M^1 k_0^{1\mathrm{S}} \xi_0^{1\mathrm{S}}(1 - R^{\mathrm{SS}}) \\ &\quad = \sqrt{\varepsilon} M^2 k_0^{2\mathrm{F}} \xi_0^{2\mathrm{F}} T^{\mathrm{SF}} + \frac{1}{\sqrt{\gamma_\kappa}} M^2 k_0^{2\mathrm{S}} \xi_0^{2\mathrm{S}} T^{\mathrm{SS}} \end{aligned} \tag{99}$$

As in the previous subsection, we seek asymptotic expressions for the transmission and reflection coefficients in the form (79) limiting our analysis by the two leading terms only. Putting $\varepsilon = 0$ yields:

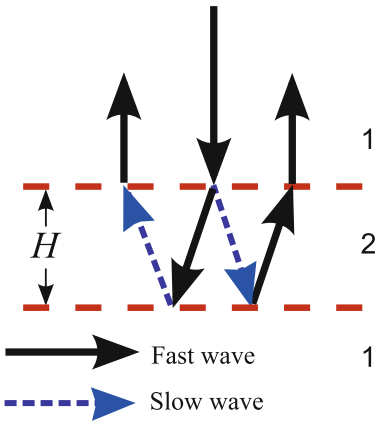

Fig. 4 Reflection from a permeable layer of type 2 sandwiched between media of type 1. A fast incident wave generates two coherent reflected fast wave

$$R_0^{SS} = \frac{-\chi_0^{1S}\frac{1}{\sqrt{\gamma_\kappa}}M^2 k_0^{2S}\xi_0^{2S} + \chi_0^{2S}M^1 k_0^{1S}\xi_0^{1S}}{\chi_0^{1S}\frac{1}{\sqrt{\gamma_\kappa}}M^2 k_0^{2S}\xi_0^{2S} + \chi_0^{2S}M^1 k_0^{1S}\xi_0^{1S}} \tag{100}$$

$$T_0^{SS} = \frac{\chi_0^{2S}\frac{1}{\sqrt{\gamma_\kappa}}M^2 k_0^{2S}\xi_0^{2S} + \chi_0^{1S}M^1 k_0^{1S}\xi_0^{1S}}{\chi_0^{1S}\frac{1}{\sqrt{\gamma_\kappa}}M^2 k_0^{2S}\xi_0^{2S} + \chi_0^{2S}M^1 k_0^{1S}\xi_0^{1S}} \tag{101}$$

Hence, using Eqs. 96 and 98, we obtain

$$R_0^{SF} = \frac{Z_2(-1 - R_0^{SS} + T_0^{SS})}{Z_1 + Z_2}, \quad T_0^{SF} = \frac{-Z_1(-1 - R_0^{SS} + T_0^{SS})}{Z_1 + Z_2} \tag{102}$$

Equations 80–81 show that a fast incident wave generates reflected and transmitted slow waves of the first order in ε. On the contrary, by virtues of equations (102), the slow and the fast waves generated by a slow incident wave are both of the zero order.

5 Reflection from a Permeable Layer

Consider reflection of a fast incident wave from a permeable layer of thickness H. Let this layer, labeled by the superscript^2, be sandwiched between two media whose properties will be labeled by the superscript^1, Fig. 4.

Both at the top and at the bottom of the layer, an incident wave generates two pairs of transmitted and reflected slow and fast waves. We consider two signals generated by reflection of an incident fast wave from the layer. In the first case, the signal is transmitted into the layer as a slow wave, reflected from the bottom of the layer as a fast wave, and further transmitted back into the upper medium 1 as a fast wave. In the second case, the signal is transmitted into the layer as a fast wave, reflected from the bottom as a slow wave, and transmitted into the upper medium as a fast wave. Figure 4 shows schematically the path of the signal for each of the two configurations. In both cases, the slow wave constitutes only one of the four segments of the whole path. Since the fast wave reflections from the top and bottom of the layer cancel each other, the considered paths generate reflected signals neglecting multiple reflections.

Both paths are similar to each other, so we consider in detail only the first one.

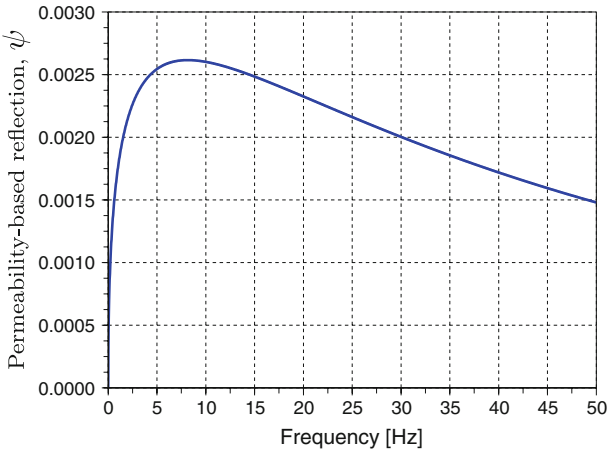

Fig. 5 The permeability-based reflection factor ψ, Eq. 105, attains a peak value at a low seismic frequency

Let U_0 be the amplitude of the incident fast wave. Then, by virtue of Eqs. 80 and 85, the amplitude of the transmitted slow wave inside the layer is equal to $U_0^{1_f 2_s} = T_1^{FS}\sqrt{|\varepsilon|}U_0$. The amplitude of the fast wave reflected from the bottom of the layer is equal to

$$U_0^{1_f 2_s 2_f} = R_0^{SF} T_1^{FS}\sqrt{|\varepsilon|}e^{-a_{SH}}U_0 \tag{103}$$

The exponential function in the last equation comes from the slow-wave attenuation. The fast-wave attenuation factor, a_F, is small of higher order relative to a_S, see Eq. 42. Note that the indices 1 and 2 must be permutated in the left equation (102) for a correct evaluation of the reflection coefficient from the bottom R_0^{SF}. Finally, for the amplitude of the signal reflected from the layer, one obtains the following expression through the amplitude of the original incident wave:

$$U_0^{1_f 2_s 2_f 1_f} = T_0^{FF} R_0^{SF} T_1^{FS}\sqrt{|\varepsilon|}e^{-a_{SH}}U_0 \tag{104}$$

For a correct evaluation of T_0^{FF}, the transmission coefficient for the signal reflected from the bottom and crossing the top interface, the indices 1 and 2 must be permutated in Eq. 81. Using Eq. 44, the ε-dependent factors in the product on the right-hand side of Eq. 104 can be gathered in the form:

$$\psi(|\varepsilon|) = \sqrt{|\varepsilon|}e^{-\frac{\eta}{\kappa}\sqrt{\frac{\gamma_\beta+\gamma_K{}^2}{2M\varrho_f}}\sqrt{|\varepsilon|}\,H} \tag{105}$$

This function is the permeability-based reflection factor. It attains a maximum value of

$$\psi_{max} = \frac{1}{H}\frac{\kappa}{\eta}\sqrt{\frac{2M\varrho_f}{\gamma_\beta+\gamma_K{}^2}}\,e^{-1} \quad \text{at } \sqrt{|\varepsilon|_{max}} = \frac{1}{H}\frac{\kappa}{\eta}\sqrt{\frac{2M\varrho_f}{\gamma_\beta+\gamma_K{}^2}} \tag{106}$$

The peak frequency is

$$\nu_{max} = \frac{\kappa}{2\pi\eta H^2}\frac{2M}{\gamma_\beta+\gamma_K{}^2} \tag{107}$$

For example, if $M = 10^{+10}$ Pa, $\gamma_\beta + \gamma_K^2 \approx 2.5$, $\kappa = 1$ Darcy, $\eta = 10^{-3}$ Pa s, and $H = 0.5$ m, then $\nu_{\max} \approx 8$ Hz, Fig. 5. This estimate is in agreement with field observations of the low-frequency gas shadow (Castagna et al. 2003).

Similarly, for the second path, the reflected signal amplitude is

$$U_0^{1_f 2_f 2_s 1_f} = T_0^{FF} R_1^{FS} T_0^{SF} \psi(|\varepsilon|) U_0 \tag{108}$$

The transmission coefficients T_0^{FF} in Eqs. 103 and 104 correspond to different direction of wave propagation through the top interface and, in general, are different.

The travel times for both paths are the same (approximately 30 ms for the numerical parameters mentioned above), as well as the peak frequencies. The phase shifts due to the travel times also are the same. Therefore, in the superposition of the reflected signals, the amplitudes (104) and (108) sum up.

5.1 Reflection from a Layered Reservoir

Due to the factor of $\sqrt{|\varepsilon|}$, the absolute value of the reflection coefficient is not large. However, frequently, a reservoir has a layered structure, where the permeability can differ between the layers by orders of magnitude. Summation of the reflections from multiple layer enhances the peak reflection effect with a noticeable time delay relative to the first arrival. In the numerical example below, such a summation produces a noticeable effect on the reflection coefficient.

For evaluation of the impedance contrasts and reflection coefficients for thick layered porous media, the conventional seismic amplitude analysis relies on Gassmann's model (Gassmann 1951). The relative easiness of assigning sensible values to the parameters in Gassmann's equation makes this model popular among exploration geophysicists (Hilterman 2001). In case of thin-layered heterogeneous reservoir, especially with significant variation of the porosity and permeability of the rock between the layers, the situation may be different. At the end of Sect. 3, we have demonstrated that Gassmann's equation can be obtained as the zero-frequency limit of the asymptotical solution obtained in the same section.

To evaluate the influence of the first-order terms on the reflection coefficients from a thin-layered reservoir, we consider a model of a 22-m thick reservoir consisting of 22 one-meter thick layers of different porosities and permeabilities. Figure 6a shows a plot of the computed fast-wave reflection coefficient, R, versus two-way travel time from reservoir surface. The calculation accounts for the multiple reflections and the fast-slow and slow-fast wave conversions at the interfaces, using Eqs. 80–81, 85–89, and 100–102. There is remarkable 10% difference between the result of application of asymptotic analysis and the result of calculation based solely on the zero-order terms (Gassmann's model), see Fig. 6b. This difference is due the first-order terms in the expressions for asymptotic reflection coefficients and it is a product of the fluid motion relatively skeleton.

6 Summary and Conclusions

A review of the derivation of Biot's equations of poroelasticity from the basic principles: momentum and mass balance equations, Hooke's law, and Darcy's law, suggests new physical interpretations for some coefficients of the classical poroelasticity. For example, the Biot-Willis coefficient α is related to the distribution of the surface of the grains between grain-to-grain and grain-to fluid contact.

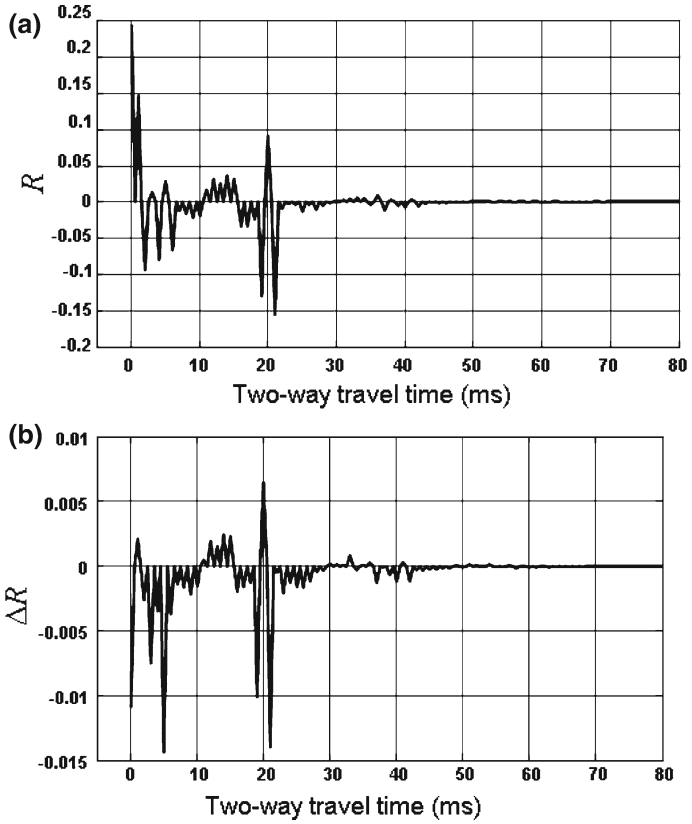

Fig. 6 Example of an inhomogeneous 22-m thick layered reservoir model. **a** Reflection coefficient R computed using Eqs. 80–81, 85–89, and 100–102 versus two-way travel time from the reservoir surface. **b** The difference $\triangle R$ between R and the reflection coefficients evaluated from the zero-order approximation (Gassmann's model)

Asymptotic analysis of a plane-wave solution at low frequencies leads to explicit relatively simple expressions for the velocity and attenuation of the fast and slow waves. The small parameter is a dimensionless quantity proportional to the product of the fluid mobility, density, and the frequency of the signal. The wave number, velocity, and attenuation factor are expressed as power series with respect to this parameter. The calculations yield that all the coefficients in the power series depend on the mechanical properties of the medium, but neither on the fluid mobility nor on the signal frequency.

The obtained asymptotic solutions lead to power-series expressions of the reflection and transmission coefficients for an elastic compression wave normally crossing a permeable planar interface between two media. It turns out that the leading frequency-dependent term is proportional to the square root of the frequency of the signal. The zero-order terms have been expressed through the acoustic impedances of the media, similarly to the classical theory.

Analysis of the reflection coefficient from a permeable layer (a lens) shows that the reflection of an incident fast wave including one slow-wave segment inside the layer is frequency-dependent and has a peak. The asymptotic relationships make possible an explicit evaluation of the maximum reflection coefficient and the peak-reflection frequency. For a realistic set of parameters, the maximum is attained at a low seismic frequency. Although the

amplitude of the reflected signal is proportional to the absolute value of the small parameter and is small, the reflection from a number of such lenses can produce a noticeable effect. Such frequencies have been successfully used for imaging the most permeable areas of a hydrocarbon-bearing reservoir (Goloshubin et al. 2006, 2008). The results of asymptotic analysis have been applied for numerical evaluation of the reflection coefficient in a model of layered reservoir with variable permeability. Calculations with account for multiple reflections show a significant contribution of the frequency-dependent part of the asymptotic expansion. The practical applications of the theory developed here are seismic modeling, inversion, and attribute analysis.

Acknowledgments This study has been performed at Lawrence Berkeley National Laboratory (LBNL) of the U.S. Department of Energy (DOE) under Contract No. DE-AC02-05CH11231, and at the University of Houston. It has been partially supported by DOE grant DE-FC26-04NT15503, the UCOil Consortium, and the Reservoir Quantification Laboratory at the University of Houston. The authors are thankful to Dr. Steven Pride and Dr. Andrea Cortis of LBNL for reviewing an early version of the manuscript and for critical remarks and suggestions. The authors also acknowledge with gratitude the critical remarks and suggestions by the anonymous reviewers, which have helped to significantly improve the presentation.

References

Alishaev, M.G., Mirzadzhanzadeh, A.K.: On retardation phenomena in filtration theory. Neft i Gaz **6**, 71–74 (1975) (in Russian)

Barenblatt, G.I., Entov, V.M., Ryzhik, V.M.: Theory of Fluid Flows through Natural Rocks. Kluwer, Dordrecht (1990)

Berryman, J.G.: Elastic wave propagation in fluid-saturated porous media. J. Acoust. Soc. Am. **69**, 416–424 (1981)

Berryman, J.G.: Elastic waves in fluid-saturated porous media. In: Burridge, R., Childress, S., Papanicolau, G. (eds.) Macroscopic Properties in Disordered Media. Proceedings of a Conference Held at the Courant Institute June 1–3, 1981, vol. 154 of Lecture Notes in Physics, pp. 38–50. Springer, Berlin (1982)

Berryman, J.G.: Origin of Gassmanns equations. Geophysics **64**(5), 1627–1629 (1999)

Berryman, J.G., Wang, H.F.: Elastic wave propagation and attenuation in a double-porosity dual-permeability medium. Int. J. Rock Mech. Mining Sci. **37**, 67–78 (2000)

Biot, M.A.: Theory of propagation of elastic waves in a fluid-saturated porous solid. I. Low-frequency range. J. Acoust. Soc. Am. **28**(2), 168–178 (1956a)

Biot, M.A.: Theory of propagation of elastic waves in a fluid-saturated porous solid. II. Higher frequency range. J. Acoust. Soc. Am. **28**(2), 179–191 (1956b)

Biot, M.A.: Mechanics of deformation and acoustic propagation in porous media. J. Appl. Phys. **33**(4), 1482–1498 (1962)

Biot, M.A., Willis, D.G.: The elastic coefficients of the theory of consolidation. J. Appl. Mech. **24**, 594–601 (1957)

Brinkman, H.C.: A calculation of the viscous force exerted by a flowing fluid in a dense swarm of particles. Appl. Sci. Res. A **1**, 27–34 (1947)

Brown, R.J.S.: Connection between formation factor for electrical resistivity and fluid-solid coupling factor in Biot's equations for acoustic waves in fluid-filled porous media. Geophysics **45**, 1269–1275 (1980)

Budiansky, B.: On the elastic moduli of some heterogeneous materials. J. Mech. Phys. Solids **13**, 223–227 (1965)

Carcione, J.M.: Viscoelastic effective rheologies for modelling wave propagation in porous media. Geophys. Prospect. **46**(3), 249–270 (1998)

Carcione, J.M., Helle, H.B., Pham, N.H.: White's model for wave propagation in partially saturated rocks: comparison with poroelastic numerical experiments. Geophysics **68**, 1389–1398 (2003)

Castagna, J.P., Sun, S., Siegfried, R.W.: Instantaneous spectral analysis: detection of low-frequency shadows associated with hydrocarbons. Lead. Edge **22**(2), 120–127 (2003)

Cortis, A.: Dynamic acoustic parameters of porous media. PhD thesis, Technische Universiteit Delft, Delft, The Netherlans, May 2002
Darcy, H.: Les Fontaines de la ville de Dijon. Victor Dalmont, Paris (1856)
Deresiewicz, H., Rice, J.T.: The effect of boundaries on wave propagation in a liquid-filled porous solid: III. Reflection of plane waves at a free plane boundary (general case). Bull. Seismol. Soc. Am. **52**(3), 595–625 (1962)
Detournay, E., Chang, A.H.-D.: Comprehensive Rock Engineering: Principle, Practice and Projects, Vol II, Analysis and Design Methods, chap. 5. Fundamentals of Poroelasticity, pp. 113–171. Pergamon Press, Oxford (1993)
Dutta, N.C., Ode, H.: Seismic reflections from a gas–water contact. Geophysics **48**(02), 148–162 (1983)
Frenkel, J.: On the theory of seismic and seismoelectric phenomena in a moist soil. J. Phys. **8**(4), 230–241 (1944)
Gassmann, F.: Über die Elastizität poröser Medien. Vierteljahrscr. Nat. Ges. Zür. **96**, 1–23 (1951)
Geertsma, J., Smit, D.C.: Some aspects of elastic wave propagation in fluid-saturated porous solids. Geophysics **26**(2), 169–181 (1961)
Goloshubin, G.M., Bakulin, A.V.: Seismic reflectivity of a thin porous fluid-saturated layer versus frequency. In: 68th SEG Meeting, pp. 976–979, New Orleans (1998)
Goloshubin, G.M., Korneev, V.A.: Seismic low-frequency effects from fluid-saturated reservoir. In: SEG Meeting, Calgary (2000)
Goloshubin, G.M., Silin, D.B.: Using frequency-dependent seismic attributes in imaging of a fractured reservoir. In: SEG Meeting, Houston, TX (2005)
Goloshubin, G.M., Daley, T.M., Korneev, V.A.: Seismic low-frequency effects in gas reservoir monitoring VSP data. In: SEG Meeting, San Antonio, TX (2001)
Goloshubin, G.M., Korneev, V.A., Vingalov, V.M.: Seismic low-frequency effects from oil-saturated reservoir zones. In: SEG Meeting, Salt Lake City, Utah (2002)
Goloshubin, G.M., Korneev, V.A., Silin, D.B., Vingalov, V.M., Van Schuyver C.: Reservoir imaging using low frequencies of seismic reflections. Lead. Edge **25**, 527–531 (2006)
Goloshubin, G., Silin, D., Vingalov, V., Takkand, G., Latfullin, M.: Reservoir permeability from seismic attribute analysis. Lead. Edge **27**, 376–381 (2008)
Gurevich, B., Zyrianov, V.B., Lopatnikov, S.L.: Seismic attenuation in finely layered porous rocks: effects of fluid flow and scattering. Geophysics **62**(1), 319–324 (1997)
Gurevich, B., Ciz, R., Denneman, A.I.M.: Simple expressions for normal incidence reflection coefficients from an interface between fluid-saturated porous materials. Geophysics **69**(6), 1372–1377 (2004)
Hashin, Z.: Theory of mechanical behavior of heterogeneous media. Appl. Mech. Rev. **17**, 1–9 (1964)
Helle, H.B., Pham, N.H., Carcione, J.M.: Velocity and attenuation in partially saturated rocks: poroelastic numerical experiments. Geophys. Prospect. **51**, 551–566 (2003)
Hilterman, F.J.: Seismic Amplitude Interpretation. Number 4 in Distinguished Instructor Series. SEG/EAGE, Lindseth, RO (2001)
Hubbert, M.K.: The theory of ground-water motion. J. Geol. **48**, 785–943 (1940)
Hubbert, M.K.: Darcy's law and the field equations of the flow of underground fluids. Trans. AIME **207**(7), 222–239 (1956)
Johnson, D., Koplik, J., Dashen, R.: Theory of dynamic permeability and tortuosity in fluid-saturated porous media. J. Fluid Mech. **176**, 379–402 (1987)
Khristianovich, S.A., Kovalenko, Y.F.: On elastic drive petroleum reservoir production. Fiz.-Tekhn. Probl. Razrab. Polyezn. Iskop. **1**, 18–37 (1991)
Kosachevskii, L.I.: On the reflection of sound waves from stratified two-component media. Appl. Math. Mech. **25**, 1608–1617 (1961)
Landau, L.D., Lifschitz, E.M.: Fluid Mechanics, vol. 6 of Series in Advanced Physics. Addison-Wesley, Reading, MA (1959)
Landau, L.D., Lifschitz, E.M.: Theory of Elasticity, 3rd edn. Pergamon Press, Oxford, England (1986)
Nikolaevskii, V.N.: Geomechanics and Fluidodynamics: With Applications to Reservoir Engineering. Kluwer, Dordrecht (1996)
Nikolaevskii, V.N., Basniev, K.S., Gorbunov, A.T., Zotov, G.A.: Mechanics of Saturated Porous Media. Nedra, Moscow (1970) (in Russian)
Pelissier, M.A., Hoeber, H., van der Coevering, N., Jones, I.F. (eds.): Classics of Elastic Wave Theory. Number 24 in Geophysics Reprint Series. Society of Exploration Geophysicists, Tulsa, OK (2007)
Pride, S.R.: Relationships between seismic and hydrological properties. In: Rubin, Y., Hubbart, S. (eds.) Hydrogeophysics, Chap. 9, pp. 253–291. Springer, NY (2005)
Pride S.R., Berryman J.G.: Linear dynamics of double-porosity dual-permeability materials. I. Governing equations and acoustic attenuation. Phys. Rev. E **68**(3), 036603-1–10 (2003a)

Pride, S.R., Berryman, J.G.: Linear dynamics of double-porosity dual-permeability materials. II. Fluid transport equations. Phys. Rev. E **68**(3), 036604-1–10 (2003b)

Pride, S.R., Garambois, S.: Electroseismic wave theory of Frenkel and more recent developments. J. Eng. Mech. **131**(9), 898–907 (2005)

Silin, D.B., Korneev, V.A., Goloshubin, G.M., Patzek, T.W.: Low-frequency asymptotic analysis of seismic reflection from a fluid-saturated medium. Transp. Porous Media **62**(3), 283–305 (2006)

Vikhorev, A. A., Ammerman, M., Chesnokov, E.M.: Reflection of elastic waves in the layered Biot medium. In: Abousleiman, Y.N., Cheung, A.H.-D., Ulm, F.-J.(eds.) Poromechanics III Biot Centennial (1905–2005) Proceedings of the 3rd Biot Conference on Poromechanics 24–27 May 2005, Norman, Oklahoma, USA, Taylor & Francis (2005)

Wei, X., Zhang, Y., Cao, L., Wang, Y., Zhang, Y.: The gradient of the amplitude spectrum of seismic data and its application in reservoir prediction. In: 2009 SEG Meeting, pp. 1102–1106, Houston, TX, October (2009)

White, J.E.: Underground Sound. Applicatiuon of Seismic Waves. Elsevier, Amsterdam (1983)